Multi-Parameter Optical Fiber Sensing of Humidity, CH_4, CO_2, and Corrosion

Badri Mainali
Research Scientist/NETL Support Contractor

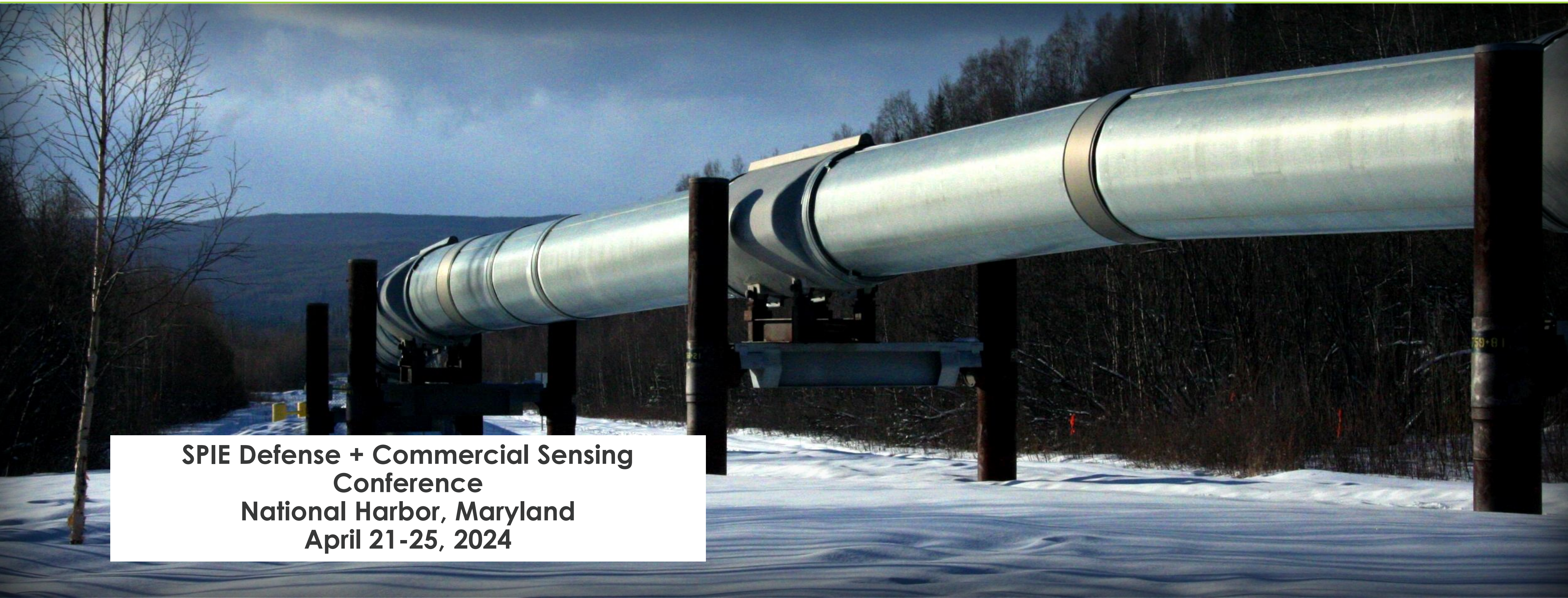

SPIE Defense + Commercial Sensing Conference
National Harbor, Maryland
April 21-25, 2024

Disclaimer

This project was funded by the United States Department of Energy, National Energy Technology Laboratory, in part, through a site support contract. Neither the United States Government nor any agency thereof, nor any of their employees, nor the support contractor, nor any of their employees, makes any warranty, express or implied, or assumes any legal liability or responsibility for the accuracy, completeness, or usefulness of any information, apparatus, product, or process disclosed, or represents that its use would not infringe privately owned rights. Reference herein to any specific commercial product, process, or service by trade name, trademark, manufacturer, or otherwise does not necessarily constitute or imply its endorsement, recommendation, or favoring by the United States Government or any agency thereof. The views and opinions of authors expressed herein do not necessarily state or reflect those of the United States Government or any agency thereof.

Authors and Contact Information

Badri Mainali[1,2]; Alexander Shumski[1,2]; Sandeep Bukka[1,2]; Nathan Diemler[1,2]; Ruishu Wright[1]

[1]National Energy Technology Laboratory, 626 Cochran Mill Road, Pittsburgh, PA 15236, USA

[2]NETL Support Contractor, 626 Cochran Mill Road, Pittsburgh, PA 15236, USA

Outline

- **Introduction**
  - Background
  - Essence of Optical Fiber Sensing
- **Experimental**
- **Results and Discussion**
  - Monitoring Humidity with Change of Microstrain in N_2
  - Monitoring Humidity with Change of Microstrain in CH_4, CO_2, and Mixed Gas Composition
  - Gas Sensing
  - Statistical Data Analysis
  - Monitoring Corrosion
- **Conclusion**

Background

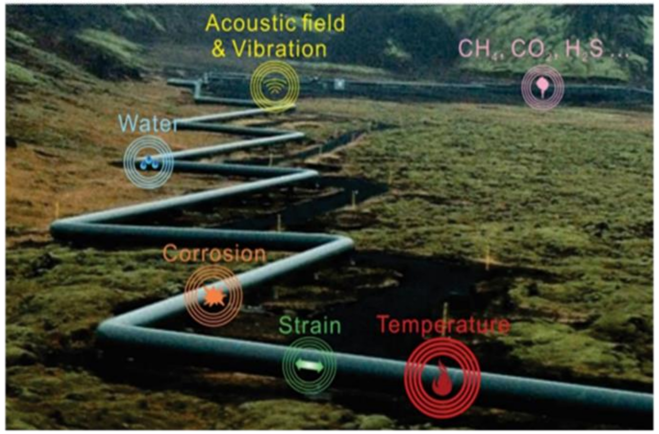

https://encryptedtbn0.gstatic.com/images?q=tbn:usqpANd
9GcTUHaf3UdOBqd3_BSU3W_HmTlDeeGxWRChMUw&

Sensors **2019**, 19, 3964

- Annual loss of ~$14.0 billion occurs in the domestic oil and gas sector due to corrosion across pipelines and exploration.
- Monitoring of corrosion requires identification and quantification of factors such as water, CO_2, and H_2S which cause corrosion.
- Conventional monitoring techniques identify leaks and events once they have occurred but are limited in capability to identify failures before they occur.
- Real-time monitoring is needed to detect and mitigate pipeline risks.

Optical Fiber Sensing

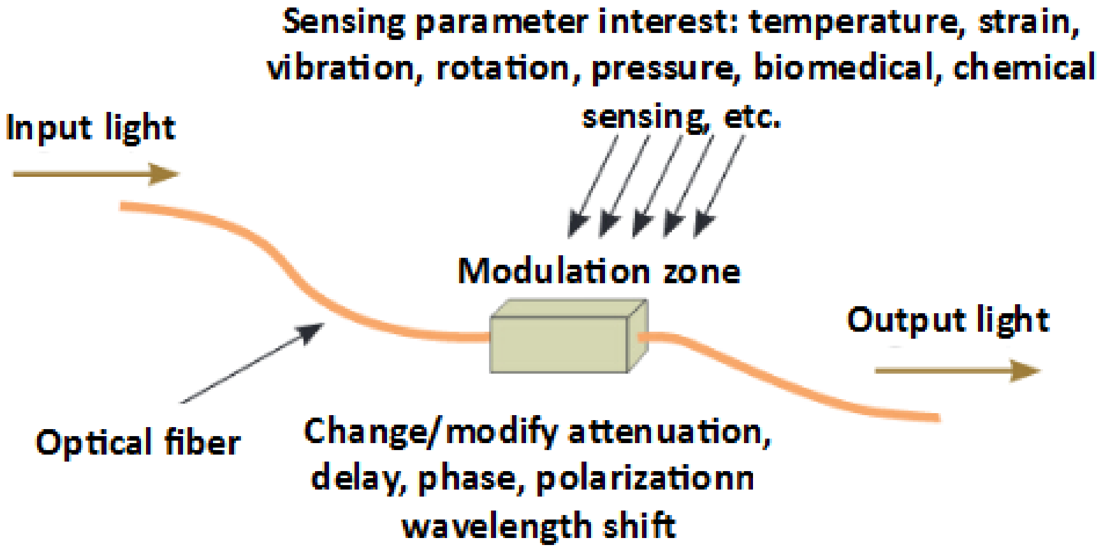

Advantages of Optical Fiber Sensing (OFS)

- Capable of nondestructive and in-situ distributed measurement
- Small size, light weight, and flexibility
- High sensitivity and accuracy
- Improved safety in the presence of inflammable gases
- Inherent immunity to electromagnetic interference
- Compatible with optical fiber data communication systems

Sensors **2019**, 19, 3964
Optical Fiber Communications, Gerd Keiser, 2002

Multi-Parameter OFS for Monitoring Humidity and Corrosion

Design of OFS for humidity and corrosion sensing

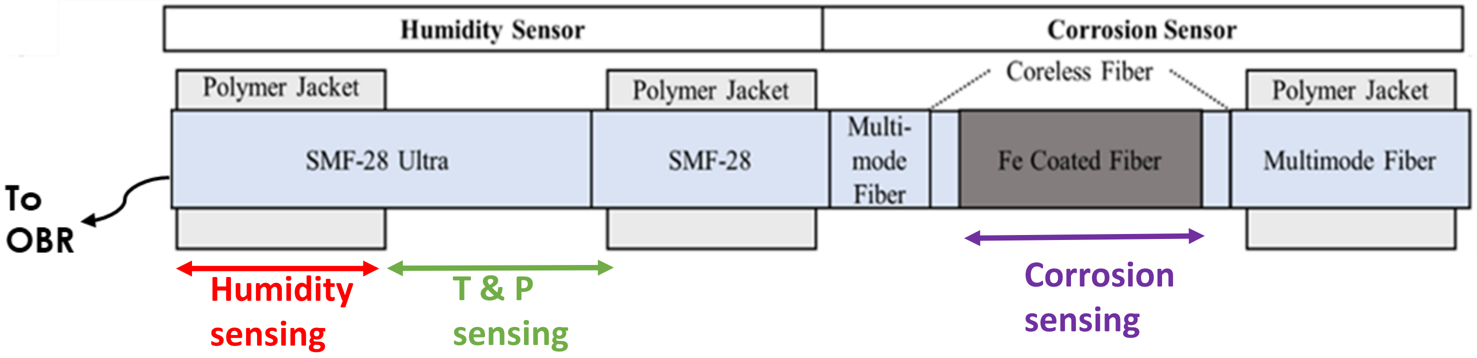

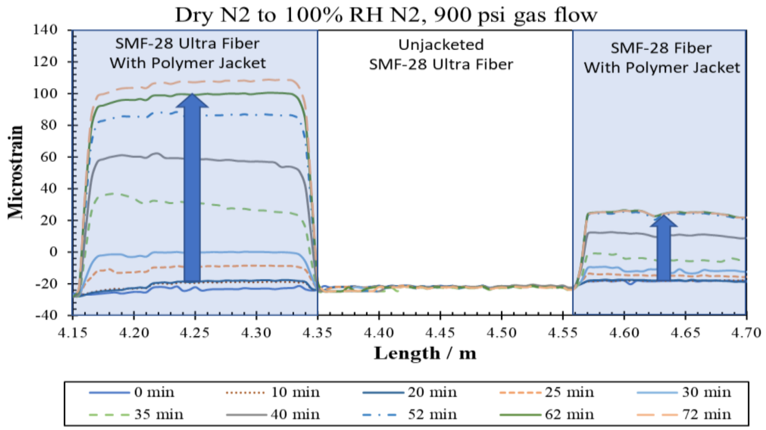

Strain-based humidity sensing using single-mode fiber (SMF) interrogated with optical backscattered reflectometer (OBR)

- Jacketed SMF-28 ultra fiber undergoes swelling upon absorption of H_2O resulting strain development
- Humidity is monitored based on the strain developed along the jacketed SMF
- Unjacketed SMFs are insensitive to humidity but sensitive to temperature (T) and pressure (P)

Proc. of SPIE Vol. 11000 1100007-5

Corrosion Sensing

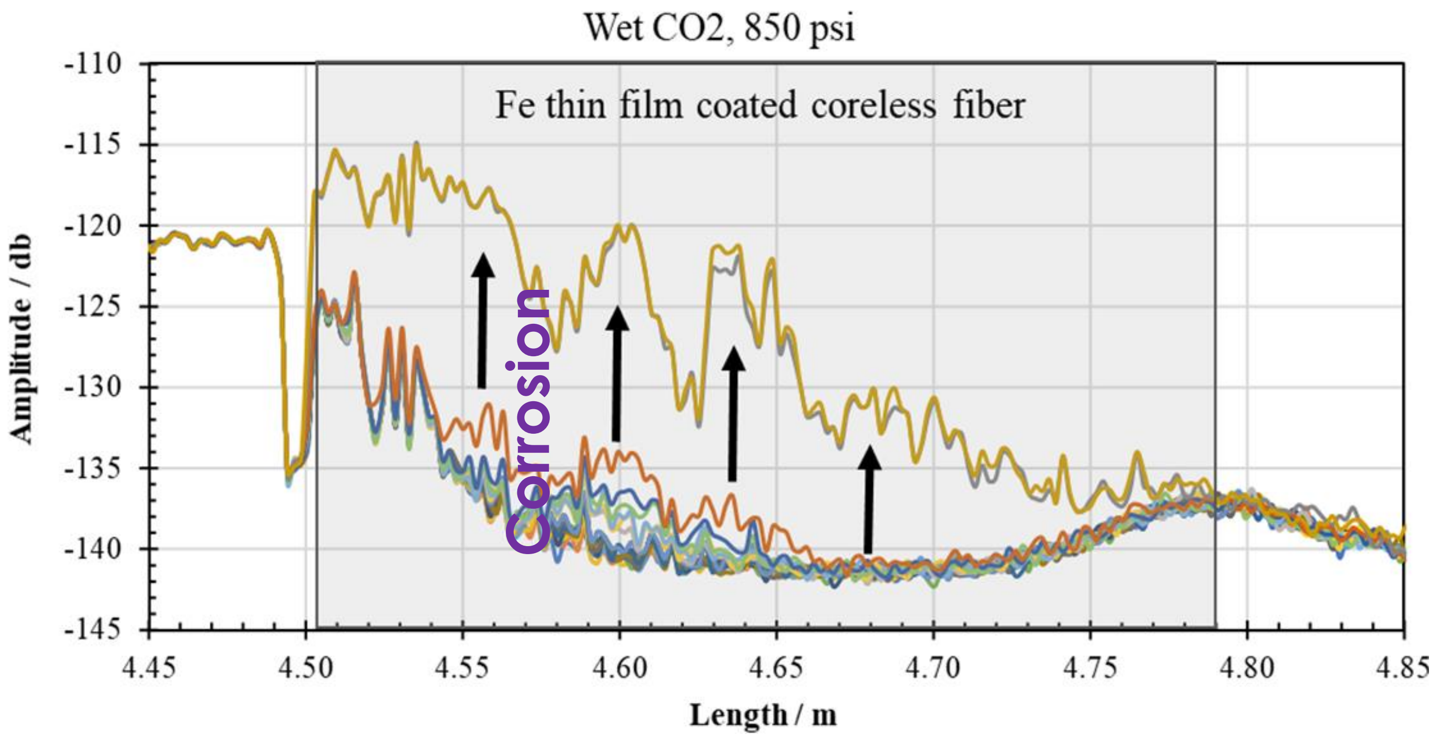

Backscattered light intensity amplitude along the Fe thin film-coated coreless fiber section in wet CO_2 gas.

- Fe undergoes corrosion/oxidative dissolution when exposed to corrosive environment (e.g., dissolved CO_2)

Anode:

$$Fe_{(s)} \longrightarrow Fe^{2+}{}_{(aq)} + 2e^-$$

Cathode:

$$2CO_{2(aq)} + 2H_2O_{(l)} + 2e^- \longrightarrow H_{2(g)} + 2HCO_3^-{}_{(aq)}$$

$$2H^+{}_{(aq)} + 2e^- \longrightarrow H_{2\,(g)}$$

- Corrosion is monitored based on the change in backscattered light intensity amplitude before and after corrosion of Fe as corrosion proxy

Proc. of SPIE Vol. 11000 1100007-5

Key Objectives and Experimental Setup-I

Objective A: Extending the capability of the OFS for calibrating strain response of SMF under controlled humidity and gas composition conditions

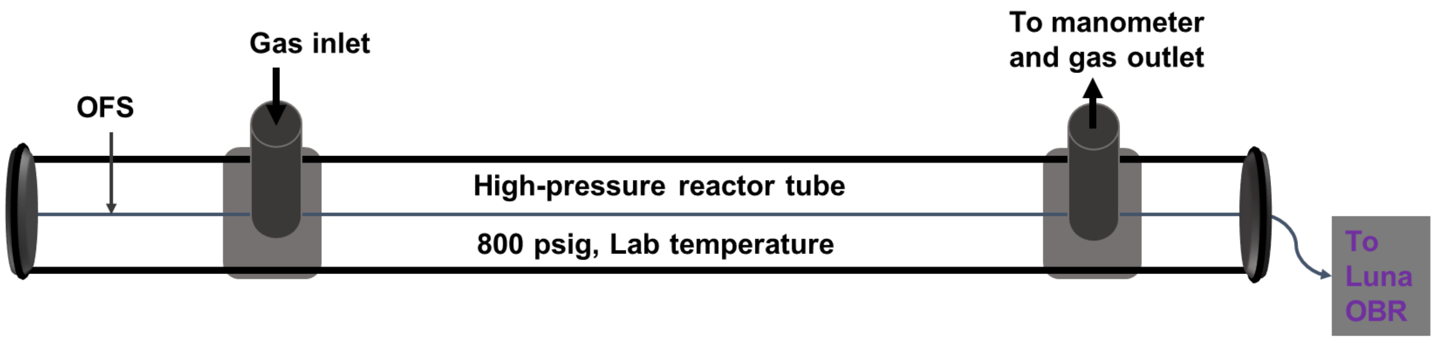

- Humidity was maintained by controlled dilution of 100% humid gas (N_2, CH_4, or CO_2) with respective dry gas (verified by humidity sensor)

  RH% studied: 100, 75.0, 46.8, and 23.4%

- Gas composition was maintained by proportional mixing of the respective gases based on their partial pressures (as mentioned subsequently)

Key Objectives and Experimental Setup-II

Objective B: Extending the capability of the Fe coated OFS for monitoring corrosion rate under harsh corrosive environment

Design of OFS for monitoring corrosion

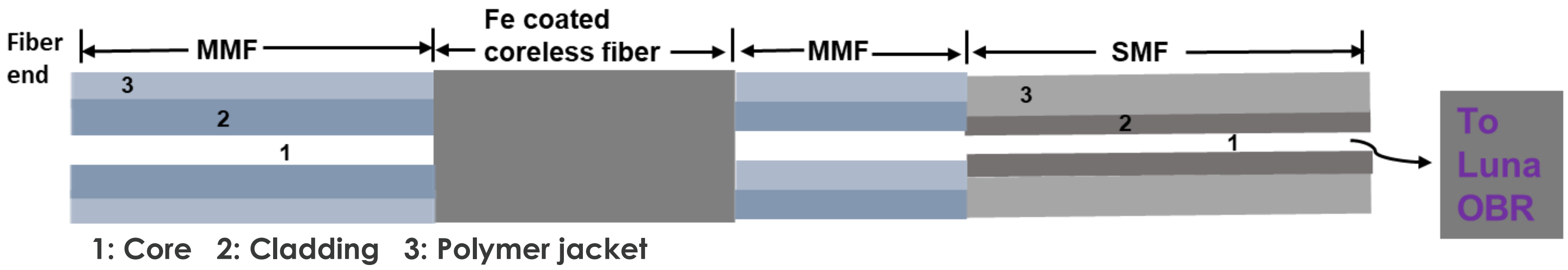

- Electroless coating of Fe onto the coreless fiber section with controlled film thickness (~25-225 nm)
- Corrosion was studied in CO_2 saturated 3.5% aq. NaCl + HCl, pH = 3.2
- Corrosion rate of Fe = $\dfrac{\text{Fe film thickness (nm)}}{\text{Time for attaining steady state backscattered intensity amplitude of the light upon complete corrosion of Fe (min)}}$

Monitoring Microstrain with Humidity in N_2

Microstrain with time in 100% RH N_2

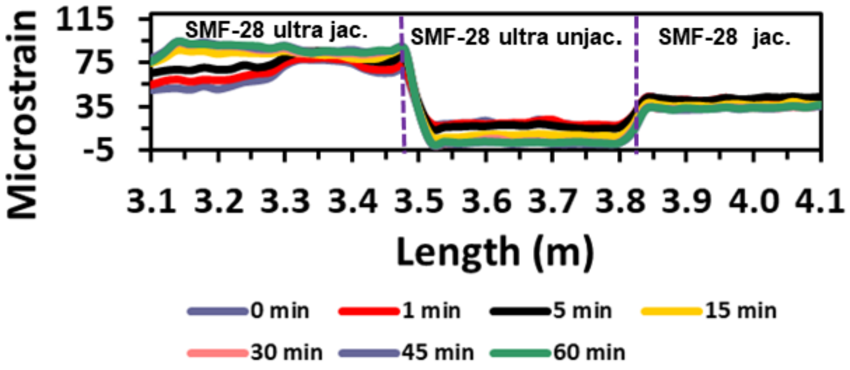

Reference trace: 800 psig dry N_2

Microstrain with change in RH%

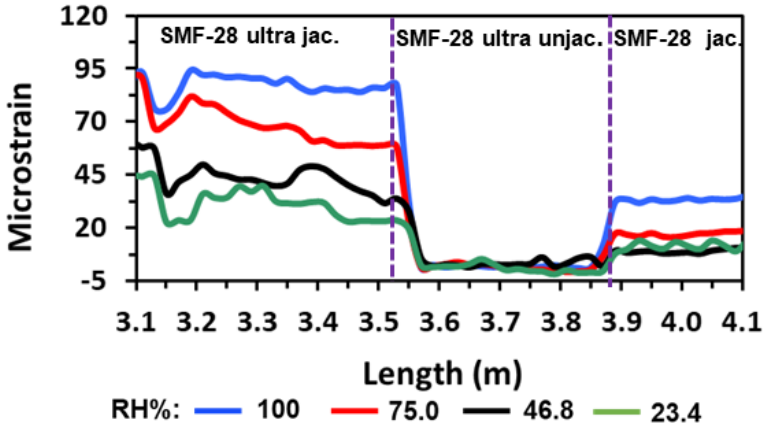

- Microstrain was measured under equilibrium (1 hr)
- Microstrain increases with increasing RH%

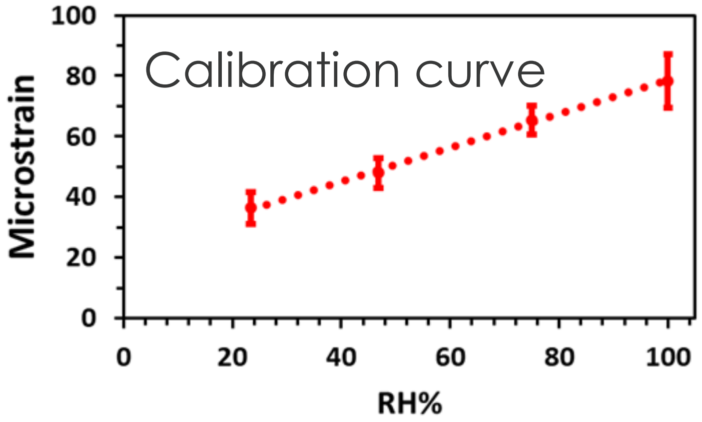

- Calibration curve shows good linear response of microstrain ($R^2 = 0.998$) with RH% change

Monitoring Microstrain with Humidity in CO_2 and CH_4

Microstrain with change in RH% in CO_2

Microstrain with change in RH% in CH_4

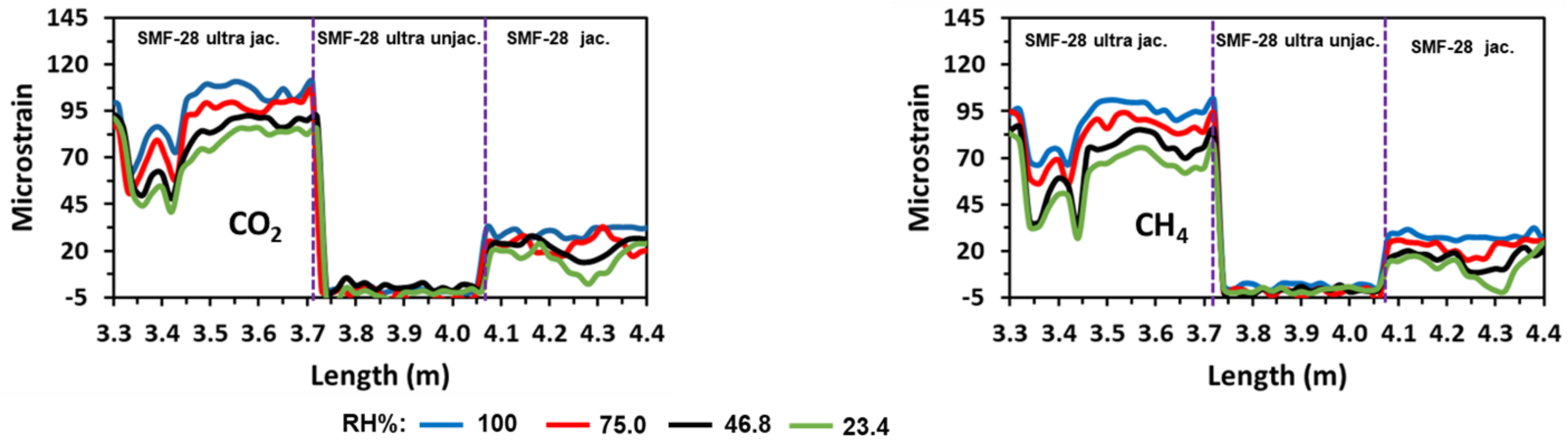

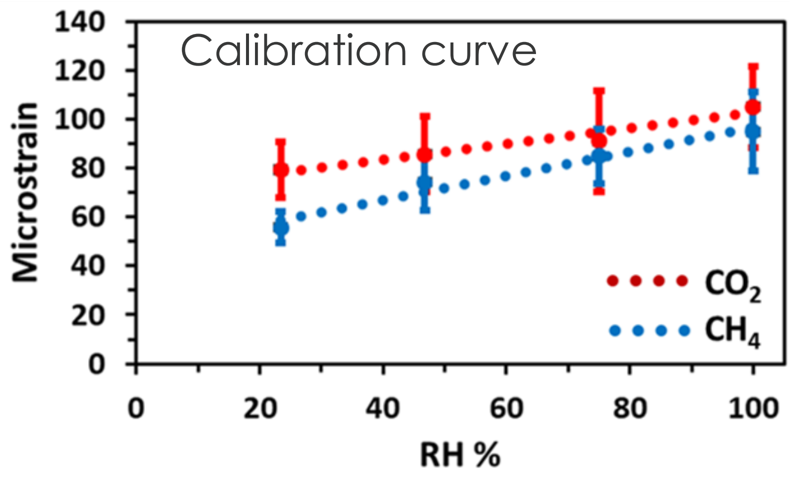

- Microstrain increases with increasing RH% in both CO_2 and CH_4
- Calibration plot shows good linear response of microstrain with RH% change:
  $R^2 = 0.967$ for CO_2, $R^2 = 0.943$ for CH_4

CO_2 Sensing

Microstrain with change in dry CO_2 concentration

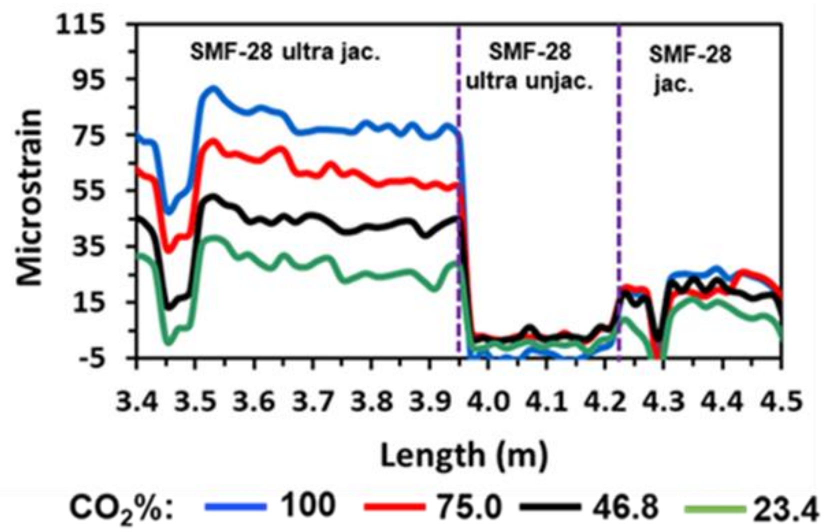

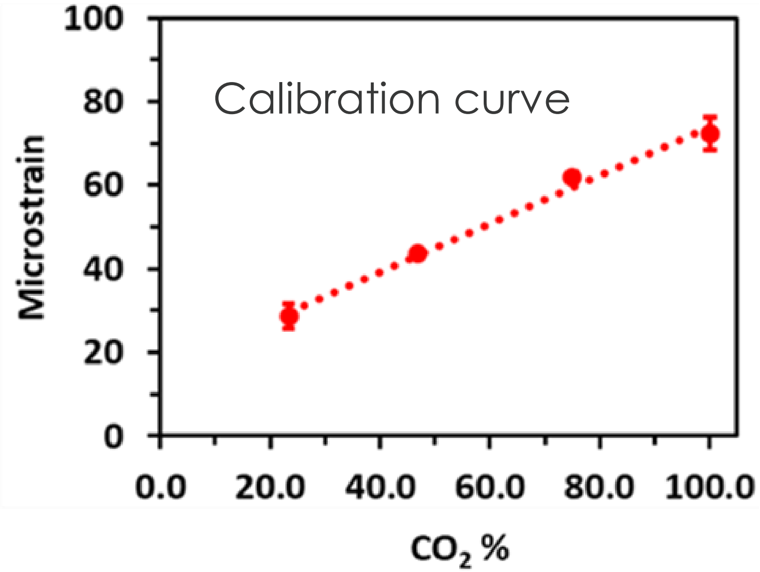

- CO_2 absorption along SMF-28 ultra causes microstrain change
- Increasing CO_2 concentration in $CO_2 + N_2$ mixture leads to an increase in microstrain
- A good linearity ($R^2 = 0.992$) between microstrain and CO_2 concentration

Microstrain Under Controlled Conditions

Microstrain measured under relative humidity and gas composition conditions at 800 psig (Reference trace: 800 psig dry N_2)

RH%	Microstrain Under								
	N_2 Composition(%)	CH_4 Composition Mixed with N_2(%)				CO_2 Composition Mixed with N_2(%)			
	100	23.4	46.8	75.0	100	23.4	46.8	75.0	100
0	0	13.2	16.9	22.9	26.0	28.8	43.5	62.0	72.4
23.4	36.4	41.5	42.0	49.9	55.8	63.8	59.8	63.1	79.4
46.8	48.0	46.7	61.7	-	74.3	53.7	74.0	-	85.8
75.0	65.4	69.9	-	74.5	85.0	69.2	-	82.5	91.1
100	78.3	-	-	-	94.9	-	-	-	105.2

Microstrain Under Mixed Gas Composition	
Gas composition	Microstrain
25% RH N_2 + 25% dry CH_4 + 50% dry CO_2	70.1
25% RH N_2 + 50% dry CH_4 + 25% dry CO_2	63.0
50% RH N_2 + 25% dry CH_4 + 25% dry CO_2	61.1
25% dry CH_4 + 75% dry CO_2	64.0
50% dry CH_4 + 50% dry CO_2	55.2
75% dry CH_4 + 25% dry CO_2	39.1

Microstrain Dataset

Microstrain at different mole fraction (X) of H_2O, N_2, CH_4, and CO_2

X_{H2O}	X_{N2}	X_{CH4}	X_{CO2}	Microstrain	X_{H2O}	X_{N2}	X_{CH4}	X_{CO2}	Microstrain
0.01165	0.9886	0	0	36.4	0	0.2501	0	0.7502	62.0
0.01165	0.7567	0.2308	0	41.3	0	0	0	1	72.4
0.01165	0.5258	0.4628	0	42.0	0.01165	0.9884	0	0	36.4
0.01165	0.2469	0.7417	0	49.9	0.01165	0.7567	0	0.2308	61.0
0.01165	0	0.9886	0	53.6	0.01165	0.5258	0	0.4628	59.8
0.02319	0.9886	0	0	48.0	0.01165	0.2469	0	0.7417	63.1
0.02319	0.7481	0.2287	0	46.7	0.01165	0	0	0.9886	81.2
0.02319	0.5557	0.4574	0	60.4	0.02319	0.7481	0	0.2287	53.7
0.02319	0	0.9768	0	74.3	0.02319	0.5557	0	0.4574	74.5
0.03719	0.9629	0	0	65.4	0.02319	0.5119	0	0.4510	85.8
0.03719	0.7374	0.2255	0	69.9	0.03719	0.7374	0	0.2255	69.2
0.03719	0.5119	0.4510	0	73.8	0.03719	0.5119	0	0.4510	83.5
0.03719	0.2576	0.7225	0	85.0	0.03719	0.2576	0	0.7225	91.1
0.04959	0.9501	0	0	78.3	0.04959	0	0	0.9501	105.2
0.04959	0	0.9501	0	94.9	0.01240	0.2469	0.2469	0.4937	70.1
0	0.7663	0.2340	0	13.2	0.01240	0.2469	0.4937	0.2469	63.0
0	0.5322	0.4681	0	16.9	0.02319	0.4884	0.2437	0.2437	61.1
0	0.2501	0.7502	0	22.9	0	0	0.2501	0.7502	64.0
0	0	1	0	26.0	0	0	0.5002	0.5002	55.1
0	0.7663	0	0.2340	28.8	0	0	0.7502	0.2501	39.1
0	0.5322	0	0.4681	43.5	-	-	-		-

Statistical Analysis of Microstrain Dataset

NATIONAL ENERGY TECHNOLOGY LABORATORY

Table: Summary of Linear Regression Analysis (n=41)

Independent Variable	Coefficients	Standard Error (%)	t-Stat	P-Value	Linearity
H_2O	a = 1176.5	6.4	15.5	8.81×10^{-18}	$R^2 = 0.959$
N_2	b = 21.8	13.2	7.60	5.09×10^{-9}	
CH_4	c = 37.3	7.9	12.7	6.43×10^{-16}	
CO_2	d = 67.9	3.1	21.8	9.96×10^{-23}	

$$a*H_2O + +b*N_2 + c*CH_4 + d*CO_2 = \text{Microstrain}$$

- Order of coefficient of independent variables: $H_2O >> CO_2 > CH_4 > N_2$
- Polarity order ($H_2O >> CO_2 > CH_4 \approx N_2$)
  Molecular size ($CH_4 > CO_2 > N_2 > H_2O$) ⇉ Absorption coefficients determined
- Analysis of t-Stat and P-value provides evidence of positive correlation between microstrain and independent variables

Corrosion Sensing: Monitoring Corrosion Rate

Changes in backscattered intensity amplitude of light along Fe coated OFS section

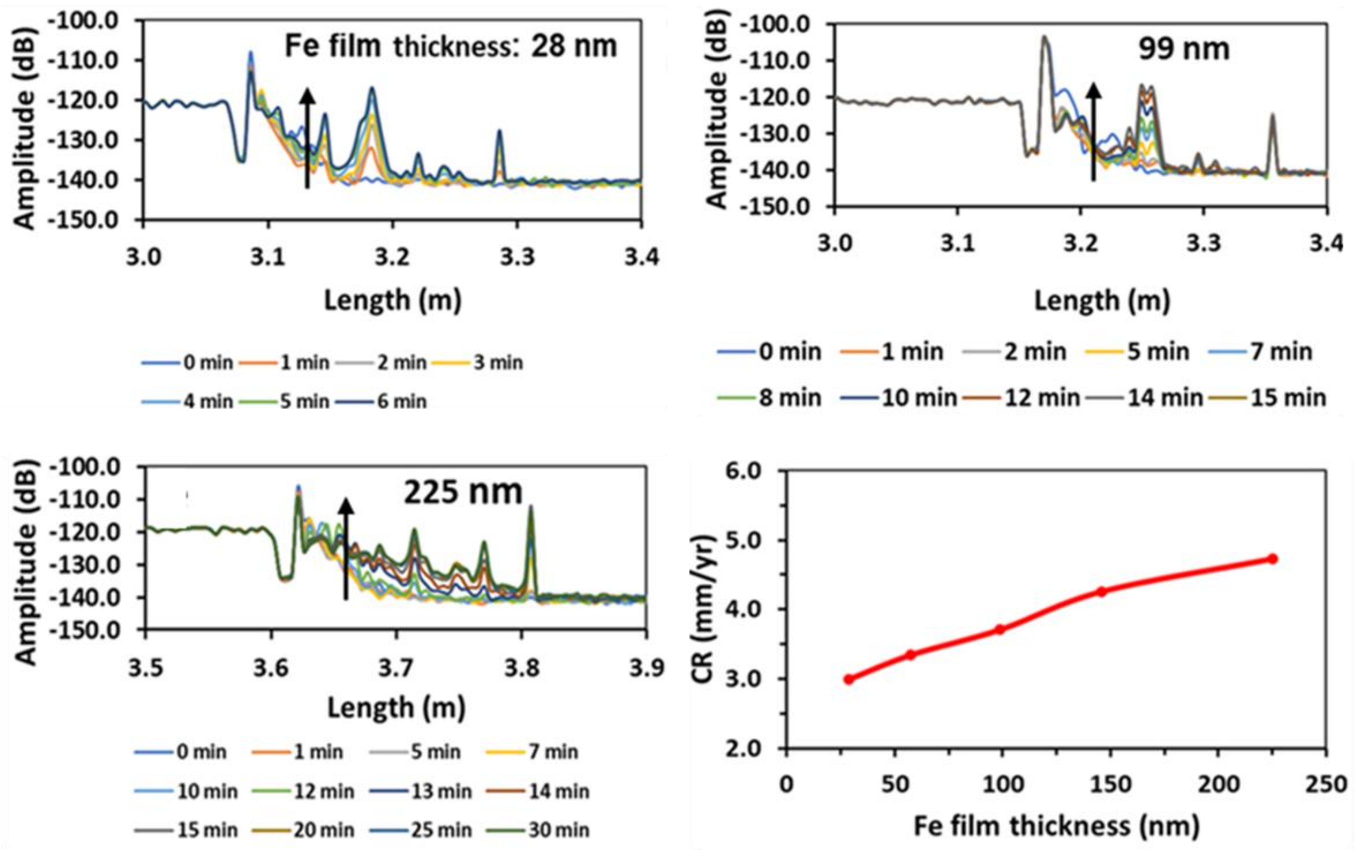

- Rate of change of Fe film thickness over time prior to reaching a steady state provides corrosion rate (CR)
- CR increases with increasing Fe film thickness possibly due to rougher film surface at higher thickness

Corrosion was studied in CO_2 saturated aqueous 3.5% NaCl + HCl, pH 3.2

Summary

- Optical fiber sensors provide long distance distributed sensing of humidity, CH_4, CO_2, and corrosion in natural gas pipeline conditions.
- Calibration shows SMF provides measurable microstrain change with a good linear response upon change in humidity and gas compositions.
- Statistical analysis reveals H_2O is the strongest contributing factor toward total strain with the order $H_2O >> CO_2 > CH_4 > N_2$ per molar unit.
- Corrosion rate was successfully monitored by using Fe coated OFS, where Fe acts as a corrosion proxy.

Acknowledgments

This work was performed in support of the U.S. Department of Energy's (DOE) Fossil Energy and Carbon Management's Natural Gas Infrastructure Program and executed through the National Energy Technology Laboratory (NETL) Research & Innovation Center' Natural Gas Infrastructure Field Work Proposal.

NETL RESOURCES

VISIT US AT: **www.NETL.DOE.gov**

@NETL_DOE

@NETL_DOE

@NationalEnergyTechnologyLaboratory

CONTACT:
Badri Mainali
Badri.Mainali@netl.doe.gov